

## Original Article

# Inner ear structure of miniature pigs measured by multi-planar reconstruction techniques

Ling-Ling Zhong<sup>1,2\*</sup>, Yan Zhang<sup>3\*</sup>, Xiao-Jie Liang<sup>4\*</sup>, Kun Hou<sup>1</sup>, Jia-Wei Han<sup>1</sup>, Fang-Yuan Wang<sup>1</sup>, Qing-Qing Hao<sup>1</sup>, Qing-Qing Jiang<sup>1</sup>, Ning Yu<sup>1</sup>, Wei-Wei Guo<sup>1</sup>, Shi-Ming Yang<sup>1</sup>

<sup>1</sup>Department of Otolaryngology, Head & Neck Surgery, Institute of Otolaryngology of PLA, Chinese PLA General Hospital, Beijing 100853, P. R. China; <sup>2</sup>Department of Otolaryngology, Head & Neck Surgery, The Tianjin Children's Hospital, Tianjin 300074, P. R. China; <sup>3</sup>Department of Otorhinolaryngology Head and Neck Surgery, The First Hospital of Jilin University, Changchun 130021, Jilin, P. R. China; <sup>4</sup>Department of Otolaryngeal-Head Neck Surgery, The Army General Hospital of PLA, Beijing 100700, P. R. China. \*Equal contributors.

Received July 28, 2017; Accepted November 21, 2017; Epub March 15, 2018; Published March 30, 2018

**Abstract:** To study the structures of the scala vestibuli and tympani of miniature pigs in order to evaluate the feasibility of using miniature pigs as the animal model for cochlear implant. The temporal bones of three miniature pigs with normal hearing were scanned by micro-CT. With the aid of the Mimics software, we reconstructed the 3D structure of inner ear basing on the serial images of the miniature pig, and obtained dimensions of the scala vestibuli and tympani with multi-planar reconstruction (MPR) technique. The constructed slicing images displayed the fine structures of the cochlea. The results of our study showed that the cross-sectional areas of the scala tympani were greatest at  $2.67 \pm 0.90 \text{ mm}^2$  when the circumferential length from the starting point of basal turn of the cochlea reached to 1.16 mm. The scala vestibuli has a largest width and height at the starting point of basal turn. The width and the height were  $2.65 \pm 0.45 \text{ mm}$  and  $2.43 \pm 0.2 \text{ mm}$  respectively. The largest width and height of the scala tympani were  $2.17 \pm 0.30 \text{ mm}$  and  $1.83 \pm 0.42 \text{ mm}$ . The result of our study suggests that the cochlea of miniature pigs is highly consistent with human's. Miniature pigs may be used as a new model for cochlear implant. MPR technique may be used as a new approach to obtain further information of patient's cochlea in surgeons which is helpful to select suitable cochlear implant devices and surgery approach.

**Keywords:** Miniature pig, cochlea, inner ear, tomography X-ray computed, image processing, MPR, cochlear implant

## Introduction

House had the metal coil implanted in the cochlea of two deaf patients, letting these two patients are able to hear the sound of the surrounding environment through a single channel electrode stimulation in 1961 for the first time. Then, Mr. F. Blair et al. started the study on the auditory nerve of the living animals and human body after cochlear implantation. As during the period from 1960s to 1970s, the study on artificial cochlea had been developed and extended in worldwide, and made great progress which included the electrical stimulation of the auditory nerve, while the single electrode and multi electrode implanted in the scala tympani [1]. With the development of half century, artificial cochlea as a treatment for severe sensorineural deafness has made remarkable achieve-

ments; however, there are still a lot of unknowns in the cochlear implantation.

Rodents, including mice [2], rats [3], guinea pigs [4, 5], and chinchillas [6], have been used for investigation on CI as animal models. What these models have in common is that their sizes of cochlea are much smaller comparing with human.

Instead that, large animal model, such as cats [7], macaques [8], sheep [9] are established for CI research. In fact, the marmoset is a perfect non-human primate model for CI research, but its usage is limited by ethics. High gene homology has made miniature pigs more feasible for ongoing in biomedical experiments, such as pharmaceutical discovery and artificial organs [10, 11]. Our earlier publications have described

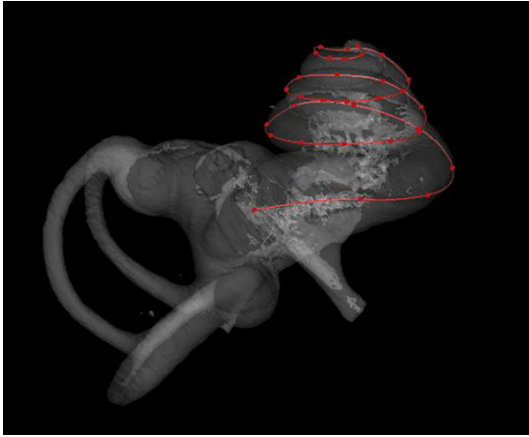


**Figure 1.** Three-dimensional reconstruction of the inner ear of the left miniature pigs' inner ear is processed through transparent model. The red line shows the cochlear length, defined as starting on the midpoint of the round window and coiling up to center line of the cochlear duct.

miniature pigs as an appropriate model in ear surgery training [12], which have very similar composition of the middle ear. Furthermore, the miniature pig has the normal hearing range and the inner ear shape after birth, which are similar with humans [13]. Since the gene homology, the anatomy of the temporal bone, and the behavioral hearing range are similar with humans, we need to investigate whether its cochlear is suitable for CI.

The cochlea is auditory organ located in petrous part of the temporal bone, surrounded by dense bone. It is composed of three parts, scala vestibuli, scala media and scala tympani. The traditional method is difficult to dissect the cochlea from the temporal bone, and more difficult to obtain the parameters inside the cochlea. Wysocki [14] and others took the method of cochlea latex perfusion to obtain the specimen of the scala vestibuli and tympani, and then the specimen was cut off and measured to get parameters of the scala vestibuli and the tympani. Li [15] took pictures of serial sections of non-staining temporal bone tissue under the microscope, and with the aid of the three-dimensional reconstruction software, the 3D structure of the scala vestibuli and the tympani was obtained, however, the relevant parameters were not obtained and measured. The flat fluorescent microscope (OPFOS) [16] and Micro-CT [17] can obtain continuous temporal images on the premise of the intact temporal

bone and gain the fine structures information within the labyrinthine. Braun [18] used the Micro-CT scan to get continuous temporal images of thickness  $5.9 \mu\text{m}$ , with the help of three-dimensional reconstruction software to reconstruct the intact cochlear structure, and segmented the scala vestibuli, scala tympani, and other fine structures within the cochlea, but comprehensive study on its dimensions was not implemented.

In recent years, researchers have been focusing on reducing the injury of cochlear implantation. "Implantation injury" was proposed by Pflugst et al [19] which refers to the injury caused as during the process of the insertion of the cochlear implant. The injury of neurons leads to the degeneration and apoptosis of neurons, which results in the loss of cell function in the end [20]. Implantation injury may cause temporary hearing loss or even permanent low frequency hearing loss [21]. Especially in patients with inner ear malformation, implantation injury is more likely to occur due to the abnormal structure of the cochlea. In addition, it also may cause implantation injury when selecting a cochlear electrode, because different electrodes have different parameters, implantation depth and hardness. The study of the fine structures of the cochlea, especially the parameters of the cochlea, has aroused great interest of us, so as to improve the safety and efficacy of cochlear implantation.

In this paper, we reconstruct the inner ear basing on high-resolution micro-CT images of the miniature pig, and obtain dimensions of the scala vestibuli and tympani by using of multiplanar reconstruction (MPR) technique with the aid of the Mimics software. We provide dimensions of the scala vestibuli and tympani along the total cochlear length of the miniature pig for the first time. The MPR technique can also provide the objective parameters for cochlear implantation, especially for the patients with inner ear malformation, and guide the surgeries to choose the more suitable implanted electrodes to reduce the implantation injury.

### Materials and methods

#### Animals

Three adult miniature pigs with normal hearing were provided by the China agricultural univer-

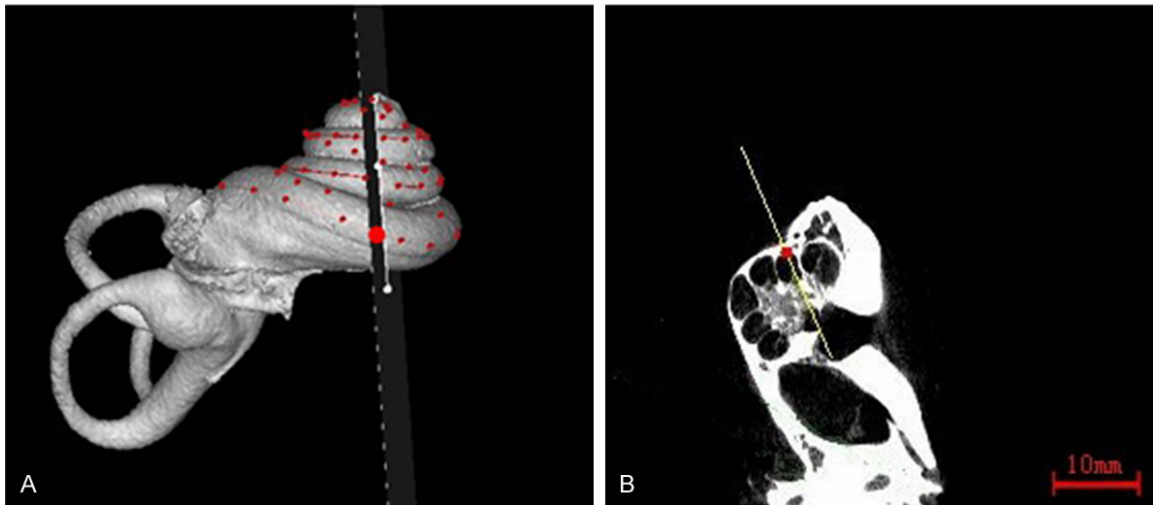


**Figure 2.** A shows the schematic of the multi-planar reconstruction technique (MPR), getting the cross-sectional image which is perpendicular to the cochlear length (B). The red dot in picture (A) indicates the reslicing position.

**Table 1.** The two measurements of CSA of the scala tympani from the beginning of the cochlear length (mm<sup>2</sup>)

Random numbers	22	17	23	35	2	22	9	6	24	3
1	0.34	0.56	0.31	0.28	3.33	0.34	1.08	1.66	0.33	2.91
2	0.32	0.56	0.32	0.27	3.30	0.34	1.10	1.67	0.34	2.91

(30 mg/kg) and xylazine (0.1 mg/kg) through muscle injection of the miniature pigs [13]. Decapitated the miniature pigs after satisfactory anesthesia quickly and obtained six halved heads. Preserved them at -20°C, and just left

them at room temperature (20°C) for thawing three hours before scanning. The use of miniature pigs was approved by the Ethical Commission of the People's Liberation Army general hospital.

#### Micro-CT scanning conditions

The six temporal bones were scanned with the X-ray microtomograph (model 1076, Skyscan, Belgium). Serial micro-CT images were taken under the scanning conditions of 91 kV, 80 μA and 200-ms exposure time [22]. Images were acquired with a slice thickness of 18 μm and 876×876 pixels. We gained 1 200 images from each specimen approximately. Fixed the specimen with the sponge and the tape to prevent artifacts during scanning.

#### Reconstruction of the inner ear and measuring the cochlear length

The micro-CT images in DICOM format were inputted into Mimics 17.0 software. The range of the selected threshold value was 220~1 100 and the results of the segmentation threshold were saved as “masks”. The masks could be edited by the software's built-in toolkit such as

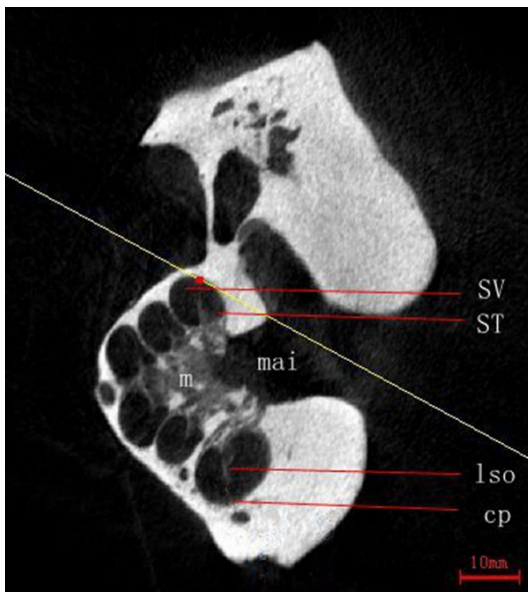


**Figure 3.** Cross-section image of the scala tympani displays fine structures within the cochlea clearly (SV, scala vestibuli; ST, scala tympani; m, modiolus; mai, meatus acusticus internus; Iso, ligamentum spiralis ossea; cp, cochlear partition).

sity (guizhou miniature pigs), without limitation of sex. Took compound anesthesia by Ketamine

## Inner ear structure of miniature pigs measured by MPR technique

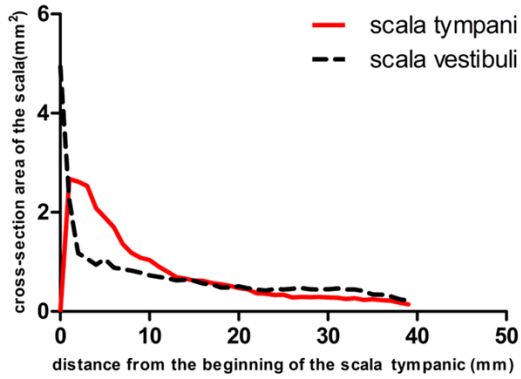


**Figure 4.** Cross-section area of the scala vestibuli and tympani along the cochlear length of the miniature pig.

calculating polylines and editing mask. Reconstructed the three-dimensional models of the inner ear.

Rotated the images of the reconstructed 3D cochlea continually and draw the center line of cochlear duct manually by the software's built-in toolkit. The cochlear length was defined as a curved line drawn from the midpoint of the round window to the terminal point of the apical turn through the center line of cochlear duct, which was consistency with Wysocki and Johnson (Figure 1).

### Reslicing images and measures of the scala

Serial images of the temporal bone inputted into the Mimics software made up the totally 3-dimensional data set. The new section image was consisted of arbitrary planar extraction from the 3-dimensional data set, which was also called the reslicing image. The "online reslice" function of the software allowed customs to obtain the parallel images across the defined curves and the parallel curves, and to get the cross-sectional images which were perpendicular to the defined curves and the parallel curves. The defined curve was set as the cochlear length (Figure 2A) and we can get the serial cross-sectional images along the cochlea coiling (Figure 2B). The "lasso" function of the software picked up the area automatically according to the similar grey value, drew the outline of the scala vestibuli and tympani accurately, and calculated the area, width and height of the corresponding region. We gained images with a slice thickness of 18  $\mu\text{m}$  from each specimen after reconstruction. We con-

ducted a measurement every 55 serial images, namely at 1 mm intervals of the cochlear length.

### Statistics

To assess the consistency of the measurements, we measured the CSA of the scala tympani in different positions of the miniature pig (numbered 1 L) again. Here, the different positions were determined by random numbers. In other words, the value of the random numbers represented the distance from the beginning of the cochlear length. Extractions of random numbers were as follows: 22, 17, 23, 35, 2, 22, 9, 6, 24, 3. The two measurements of CSA of the scala tympani were listed in Table 1 in the above-mentioned positions. A method of Bland-Altman by the MedCalc 15.0 software was used to evaluate the consistency of the measurements. The consistency interval is defined between  $d-1.96S_d$  and  $d+1.96S_d$ .

## Results

### The fine structures of the cochlea

When finished the MPR, the fine structures of the cochlea can be displayed clearly (Figure 3), including the scala vestibuli, scala tympani, modiolus, meatus acusticus internus, ligamentum spiralis ossea and cochlear partition. Cochlear partition is the compound structures which is regarded as the lamina spiralis ossea extending to the lateral wall of the cochlea, including vestibular membrane, basilar membrane and spiral ligament, dividing the cochlea into scala vestibuli and tympani [18]. In fact, the cochlea consists of three lymphatic spaces. The scala vestibuli and tympani are full of perilymph, while the scala media is filled with endolymph. Because of the resolution limitations to soft tissue of the micro-CT, the temporal bone images with a slice thickness of 18  $\mu\text{m}$  we obtained could not distinguish the vestibular membrane from basilar membrane clearly.

### The cross-sectional area of the scala

The start of the scala tympani was identified as the round window, while the scala vestibuli started from the oval window. At the beginning of the first 0.96 mm of the cochlear length, the CSA of the scala tympani increases rapidly while the scala vestibuli decreases continually. The CSA of the scala tympani is greatest (2.67



## Inner ear structure of miniature pigs measured by MPR technique

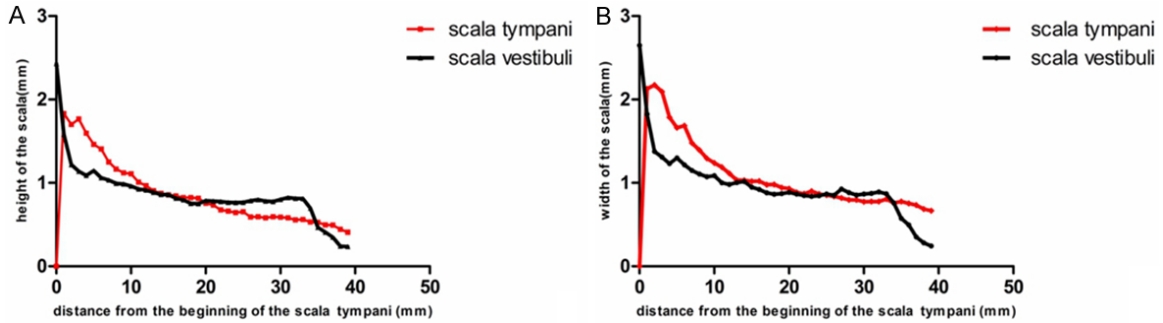


**Figure 5.** A. Height of the scala vestibuli and tympani along the cochlear length of the miniature pig. B. Width of the scala vestibuli and tympani along the cochlear length of the miniature pig.

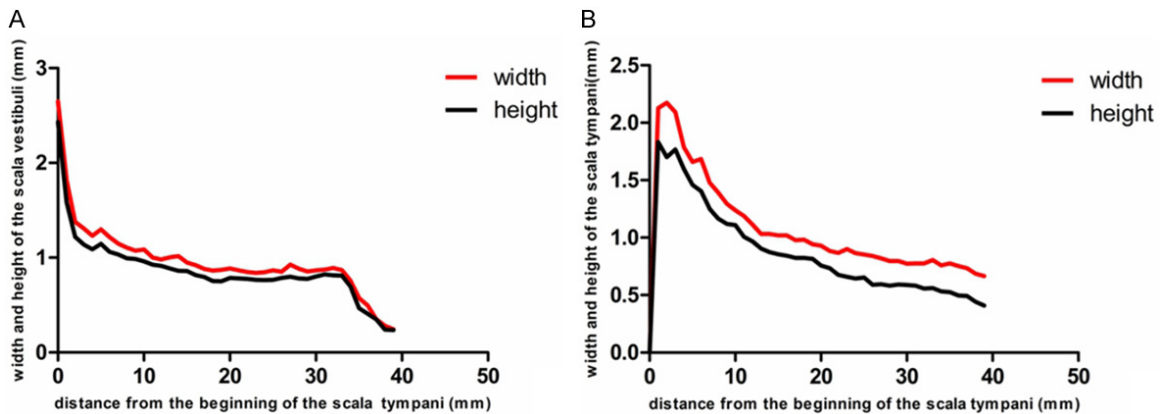


**Figure 6.** A. Width and height of the scala vestibuli along the cochlear length of the miniature pig. B. Width and height of the scala tympani along the cochlear length of the miniature pig.

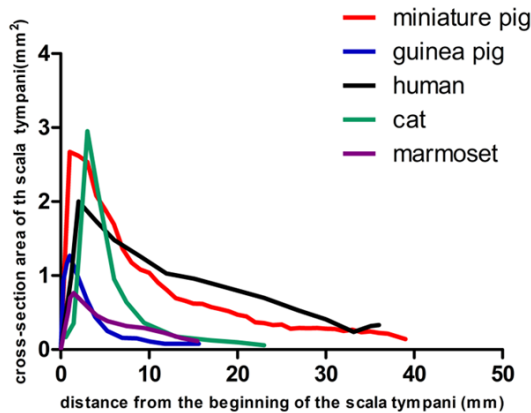


**Figure 7.** Comparison of the cross-sectional area of the miniature pig, the guinea pig, the cat, the marmoset and the human along the cochlear length.

$\pm 0.90 \text{ mm}^2$ ) at 1.16 mm from the beginning of the cochlear length. It shows that CSA of the scala tympani is larger than scala vestibuli in the first 1.16-13.60 mm. After the point of 13.60 mm, they are very close and keeping

stable relatively by contrast of these two datas (Figure 4).

### *The height and width of the scala*

Width was measured parallel to the cochlear partition where the distance within the scala was greatest. Height was also the greatest distance taken perpendicular the width measurement. **Figure 5A** shows the comparison of the height of the scala vestibuli and tympani, and **Figure 5B** shows the comparison of the width of the scala vestibuli and tympani. They have shown striking similarity. Before the first 0.90 mm of the cochlear length, the height and the width of the scala tympani are rapidly increasing, while the height and the width of the scala vestibuli are decreasing. At this stage, both the width and height of the scala vestibuli are larger than those of the scala tympani. From the 0.90 to 12.57 mm of the cochlear length, it shows a reversal result, that is, the height and the width of the scala vestibuli are rapidly increasing comparing with the decreasing scala

## Inner ear structure of miniature pigs measured by MPR technique

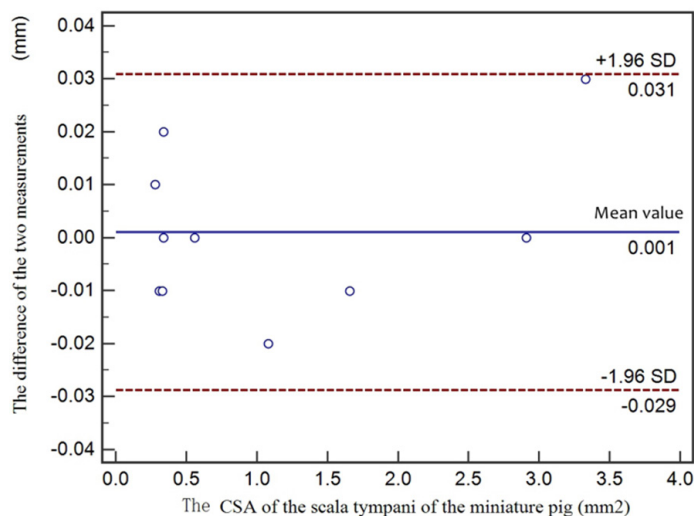


**Figure 8.** Evaluating the consistency of the measurements: the horizontal axis represents CSA of the scala tympani of the miniature pig, while the vertical axis stands for the difference of the two measurements. The two dashed lines are  $d-1.96S_d$  and  $d+1.96S_d$ , respectively.

tympani. After then, the height and width of both scala vestibuli and scala tympani reach to a stable stage.

The variation trends of the height and width of scala vestibuli and scala tympani of the miniature pig are similar. The width is larger than the height both in the scala vestibuli and tympani. The width and the height of the scala vestibuli are maximum ( $2.65 \pm 0.45$  mm,  $2.43 \pm 0.29$  mm respectively) at the starting point of the cochlear length and minimum at the ending point. The maximum of the scala tympani has a width of  $2.17 \pm 0.30$  mm and a width of  $1.83 \pm 0.42$  mm (**Figure 6A, 6B**).

### *Comparison of the CSA of the scala tympani between the experiment animals and humans*

Comparing the miniature pig, the guinea pig, the cat and the marmoset with the human (**Figure 7**), the CSA of the scala tympani of the miniature pig is obviously much close to the humans', while other animals are much smaller than human. At the beginning 6.85 mm of the cochlear length, the CSA of the miniature pig is larger than human, greatest to  $2.67+0.90$  mm<sup>2</sup>, whereas the maximum CSA of the human is 2.00 mm<sup>2</sup>. Between 0-6.85 mm of the cochlear length, the CSA of the miniature pig is larger than human, while it turns a reversal result at the phase of 6.85-33.10 mm.

It should be emphasized that the methods used for these species were inconsistent. Miniature pig as well as the marmoset [8] measures were gained basing on micro-CT. The human [14], and cat [23] measurements were taken by using of physical measurements of latex molds, while the guinea pig [24] measurements were reconstructed by using of three-dimensional MRI images.

### *Assessment the consistency of the measurements*

The horizontal axis represents CSA of the scala tympani of the miniature pig, while the vertical axis stands for the difference of the two measurements. The two dashed lines are  $d-1.96S_d$  and  $d+1.96S_d$ , respectively. The result shows that

the ten groups are all in the consistency interval, presenting great consistency of the measurements (**Figure 8**).

## Discussion

The highlight of this research is to provide a non-destructive method for fine structures of the cochlea, comparing with the latex mold technique [14] as well as the histological section technique [25]. Here, the MPR technique we introduced is not strange in the clinical application. Liu et al. [26] apply the MPR technique in measuring the cochlear length. MPR technique has obvious advantages in diagnosing the fistula of semicircular canal to display the whole semicircular canal and the position of the fistula [27]. MPR technique integrating with radiological images is expected as an accurate imaging diagnostic method for preoperative evaluation of CI.

The CI animal model we choose should have the most similar CSA parameters with humans. We compare the CSA of the scala tympani with the miniature pig, human [14] and other commonly used experimental animals (guinea pig, cat and the marmoset) [8, 23]. The results of our study show a high similarity with Wysocki [5]. The dimensions of the scala tympani (CSA, height and width) include three phases, such as fast-rising period, slow-dropping period and

plateau. The width is larger than the height along the cochlear length both in the scala vestibuli and tympani. It must be emphasized that the data used for comparison are obtained by different methods. To our surprise, the miniature pig is highly consistent with the human in the sizes of the scala tympani. Nevertheless, the comparison is provided with the reference for choosing the animal model for cochlear implantation.

McClay et al. [28] found that more than 20% patients with congenital hearing loss were associated with inner ear malformations. With the improvement of cochlear implantation technology, severe hearing loss associated with inner ear malformation is also an indication for cochlear implantation, and these patients also obtain satisfied effects more than we expected [29]. However, the abnormal structures resulted from the inner ear malformation increase more surgery difficulties and more postoperative complications of cochlear implantation. Routine imaging examinations including HRCT, MRI are used for CI patients preoperatively. The obtained images cannot reflect the actual position of the cochlea within the temporal bone. With the help of the “online reslice” function of the software, we can gain the miniature pig CSA along the cochlear length. This MPR technology is expected to be applied in CI, so as to guide surgeons to choose the most appropriate electrode and improve success of the complex cochlear implant.

In recent years, the importance of protecting the residual hearing during cochlear implantation has been recognized by otologists. The residual hearing is beneficial to improve the speech recognition in noise environment and music appreciation [30], so as to improve the quality of life in patients. The loss of residual hearing is the result of multiple factors, and the selection of implantation electrodes is just one of them [31]. Cochlear manufactures have also introduced many types of short electrodes with different length and different parameters, such as Flex24, Flex20EAS from Med-EI and Hybrid L24 from Cochlear. Compared to the Combi40+ Med-EI, CI422 Nucleus and other standard length electrodes, the short electrode has advantages of short implanted length and small electrode parameters. Although the short implanted electrode can achieve well-pleasing hearing effects in the early stage, it does not

mean that the smaller the implanted electrodes are the better hearing effects we get. Friedmann and his team [32] compared the hearing effects from the CI422 Nucleus and Hybrid L after 1-year implanting, finding that the speech recognition rate in standard implanted electrode group is better than the short implanted electrode group. Implantation injury includes the early stage and the late stage. Early injury is mainly caused by direct mechanical injury to the basilar membrane and the stria vascularis during the process of electrode insertion. The late injury is presumably caused by the results of the chronic inflammatory reaction, the formation of fibrous tissue around the electrode and ossification of the never in the scala tympani after cochlear implantation [33, 34]. The long-term mechanism of the loss of the residual hearing is unclear, but recent evidences suggest that [32, 35] choosing a suitable implanted electrode combined with minimally invasive surgical approach can reduce the implantation injury and protect the residual hearing. The residual hearing is pursued by all otologists. MPR technique provides us with detailed dimensions on the scala vestibuli and tympani, which is referenced in choosing appropriate implanted electrode.

The dimensions of the cochlea present the miniature pig as highly comparable to that of the human. This underlines the suitability of the miniature pig as an animal model for cochlear implant. The emergence of animal models provides us with conditions for research on the electrophysiology of auditory pathway from hair cells to the auditory cortex. The application of MPR technique may be a new approach to provide more detailed information of the patients to reduce the implantation injury for evaluating the structure of the inner ear, also guiding the surgeries choosing the suitable implanted electrodes.

### Acknowledgements

This work was supported by grants from the National Natural Science Foundation of China (No. 81670940, 81670941, 81570933, and 81400472), and Special Cultivating and Developing Program of Beijing Science and Technology Innovation Base (z1511000016-15050), and Army Key Projects of Scientific Research in 12th Five-Year (BWS14J045).and

the Natural Science Foundation of Jilin Province Science and Technology Department (20160101020JC).

### Disclosure of conflict of interest

None.

**Address correspondence to:** Shi-Ming Yang and Wei-Wei Guo, Department of Otolaryngology, Head & Neck Surgery, Institute of Otolaryngology, Chinese PLA General Hospital, Beijing 100853, P. R. China. Tel: +861068211696; E-mail: yangsm301@263.net (SMY); gwent001@163.com (WWG)

### References

- [1] Wilson BS, Dorman MF. Cochlear implants: a remarkable past and a brilliant future. *Hear Res* 2008; 242: 3-21.
- [2] Mistry N, Nolan LS, Saeed SR, Forge A, Taylor RR. Cochlear implantation in the mouse via the round window: effects of array insertion. *Hear Res* 2014; 312: 81-90.
- [3] Lu W, Xu J, Shepherd RK. Cochlear implantation in rats: a new surgical approach. *Hear Res* 2005; 205: 115-122.
- [4] Giordano P, Hatzopoulos S, Giarbini N, Prosser S, Petruccioli J, Simoni E, Faccioli C, Astolfi L, Martini A. A soft-surgery approach to minimize hearing damage caused by the insertion of a cochlear implant electrode: a guinea pig animal model. *Otol Neurotol* 2014; 35: 1440-1445.
- [5] Honeder C, Landegger LD, Engleder E, Gabor F, Plasenzotti R, Plenk H, Kaider A, Hirtler L, Gstoettner W, Arnoldner C. Effects of intraoperatively applied glucocorticoid hydrogels on residual hearing and foreign body reaction in a guinea pig model of cochlear implantation. *Acta Otolaryngol* 2015; 135: 313-319.
- [6] Hessel H, Ernst LS, Walger M, von Wedel H, Dybek A, Schmidt U. Meriones unguiculatus (Gerbil) as an animal model for the ontogenetic cochlear implant research. *Am J Otol* 1997; 18: S21.
- [7] Fallon JB, Shepherd RK, Nayagam DA, Wise AK, Heffer LF, Landry TG, Irvine DR. Effects of deafness and cochlear implant use on temporal response characteristics in cat primary auditory cortex. *Hear Res* 2014; 315: 1-9.
- [8] Johnson LA, Della Santina CC, Wang X. Temporal bone characterization and cochlear implant feasibility in the common marmoset (*Callithrix jacchus*). *Hear Res* 2012; 290: 37-44.
- [9] Schnabl J, Glueckert R, Feuchtner G, Recheis W, Potrusil T, Kuhn V, Wolf-Magele A, Riechelmann H, Sprinzl GM. Sheep as a large animal model for middle and inner ear implantable hearing devices: a feasibility study in cadavers. *Otol Neurotol* 2012; 33: 481-489.
- [10] Vamathevan JJ, Hall MD, Hasan S, Woollard PM, Xu M, Yang Y, Li X, Wang X, Kenny S, Brown JR, Huxley-Jones J, Lyon J, Haselden J, Min J, Sanseau P. Minipig and beagle animal model genomes aid species selection in pharmaceutical discovery and development. *Toxicol Appl Pharmacol* 2013; 270: 149-157.
- [11] Petersen B, Carnwath JW, Niemann H. The perspectives for porcine-to-human xenografts. *Comp Immunol Microbiol Infect Dis* 2009; 32: 91-105.
- [12] Yi HJ, Guo W, Wu N, Li JN, Liu HZ, Ren LL, Liu PN, Yang SM. The temporal bone microdissection of miniature pigs as a useful large animal model for otologic research. *Acta Otolaryngol* 2014; 134: 26-33.
- [13] Guo W, Yi H, Ren L, Chen L, Zhao L, Sun W, Yang SM. The morphology and electrophysiology of the cochlea of the miniature pig. *Anat Rec (Hoboken)* 2015; 298: 494-500.
- [14] Wysocki J. Dimensions of the human vestibular and tympanic scalae. *Hear Res* 1999; 135: 39-46.
- [15] Li SF, Zhang TY, Wang ZM. An approach for precise three-dimensional modeling of the human inner ear. *ORL J Otorhinolaryngol Relat Spec* 2006; 68: 302-310.
- [16] Voie AH. Imaging the intact guinea pig tympanic bulla by orthogonal-plane fluorescence optical sectioning microscopy. *Hear Res* 2002; 171: 119-128.
- [17] Shin KJ, Lee JY, Kim JN, Yoo JY, Shin C, Song WC, Koh KS. Quantitative analysis of the cochlea using three-dimensional reconstruction based on microcomputed tomographic images. *Anat Rec (Hoboken)* 2013; 296: 1083-1088.
- [18] Braun K, Böhnke F, Stark T. Three-dimensional representation of the human cochlea using micro-computed tomography data: presenting an anatomical model for further numerical calculations. *Acta Otolaryngol* 2012; 132: 603-613.
- [19] Pflingst BE, Hughes AP, Colesa DJ, Watts MM, Strahl SB, Raphael Y. Insertion trauma and recovery of function after cochlear implantation: Evidence from objective functional measures. *Hear Res* 2015; 330: 98-105.
- [20] Spoendlin H, Schrott A. Analysis of the human auditory nerve. *Hear Res* 1989; 43: 25-38.
- [21] Su GL, Colesa DJ, Pflingst BE. Effects of deafening and cochlear implantation procedures on postimplantation psychophysical electrical detection thresholds. *Hear Res* 2008; 241: 64-72.



## Inner ear structure of miniature pigs measured by MPR technique

- [22] Zhong LL, Hao QQ, Ren LL, Guo WW, Yang SM. [Establishment of a mathematical model for calculating cochlear length]. *Zhonghua Er Bi Yan Hou Tou Jing Wai Ke Za Zhi* 2016; 51: 446-450.
- [23] Wysocki J. Dimensions of the vestibular and tympanic scalae of the cochlea in selected mammals. *Hear Res* 2001; 161: 1-9.
- [24] Thorne M, Salt AN, DeMott JE, Henson MM, Henson OW Jr, Gewalt SL. Cochlear fluid space dimensions for six species derived from reconstructions of three-dimensional magnetic resonance images. *Laryngoscope* 1999; 109: 1661-1668.
- [25] Wei XF, Zhang XY, Yuan WU, Li YS. Accuracy of computer-aided geometric three-dimensional reconstruction of the human petrous bone based on serial unstained celloidin sections. *Exp Ther Med* 2015; 9: 1113-1118.
- [26] Liu YK, Qi CL, Tang J, Jiang ML, Du L, Li ZH, Tan SH, Tang AZ. The diagnostic value of measurement of cochlear length and height in temporal bone CT multiplanar reconstruction of inner ear malformation. *Acta Otolaryngol* 2017; 137: 119-126.
- [27] Yu L, Sun X, Ding Y. [The diagnostic value of labyrinthine fistula with multi-planar reconstruction in chronic otitis media by HRCT]. *Lin Chung Er Bi Yan Hou Tou Jing Wai Ke Za Zhi* 2012; 26: 16-18.
- [28] McClay JE, Tandy R, Grundfast K, Choi S, Vezina G, Zalzal G, Willner A. Major and minor temporal bone abnormalities in children with and without congenital sensorineural hearing loss. *Arch Otolaryngol Head Neck Surg* 2002; 128: 664-671.
- [29] Arnoldner C, Baumgartner WD, Gstoettner W, Egelierler B, Czerny C, Steiner E, Hamzavi J. Audiological performance after cochlear implantation in children with inner ear malformations. *Int J Pediatr Otorhinolaryngol* 2004; 68: 457-467.
- [30] Gifford RH, Dorman MF, Skarzynski H, Lorens A, Polak M, Driscoll CL, Roland P, Buchman CA. Cochlear implantation with hearing preservation yields significant benefit for speech recognition in complex listening environments. *Ear Hear* 2013; 34: 413-425.
- [31] Nguyen S, Cloutier F, Philippon D, Côté M, Bussièrès R, Backous DD. Outcomes review of modern hearing preservation technique in cochlear implant. *Auris Nasus Larynx* 2016; 43: 485-488.
- [32] Friedmann DR, Peng R, Fang Y, McMenomey SO, Roland JT, Waltzman SB. Effects of loss of residual hearing on speech performance with the CI422 and the Hybrid-L electrode. *Cochlear Implants Int* 2015; 16: 277-284.
- [33] Li PM, Somdas MA, Eddington DK, Nadol JB Jr. Analysis of intracochlear new bone and fibrous tissue formation in human subjects with cochlear implants. *Ann Otol Rhinol Laryngol* 2007; 116: 731-738.
- [34] Nadol JB Jr, Eddington DK. Histopathology of the inner ear relevant to cochlear implantation. *Adv Otorhinolaryngol* 2006; 64: 31-49.
- [35] Lenarz T, James C, Cuda D, Fitzgerald O'Connor A, Frachet B, Frijns JH, Klenzner T, Laszig R, Manrique M, Marx M, Merkus P, Mylanus EA, Offeciers E, Pesch J, Ramos-Macias A, Robier A, Sterkers O, Uziel A. European multi-centre study of the Nucleus Hybrid L24 cochlear implant. *Int J Audiol* 2013; 52: 838-848.